Neuroplasticity-Related Genes and Dopamine Receptors Associated with Regional Cortical Thickness Increase Following Electroconvulsive Therapy for Major Depressive Disorder

Gong-Jun JI [a,b,c,d#], Jiao Li [e,f#], Wei Liao [e,f#], Tongjian Bai [a,b,c,d], Ting Zhang [a,b,c,d], Wen Xie [g], Kongliang He [g], Chuyan Zhu [a,b,c,d], Juergen Dukart [h,i], Chris Baeken [j], Yanghua Tian [a,b,c,d *], Kai Wang [a,b,c,d *]

[#] These authors contributed equally to this work

[a] Department of Neurology, The First Affiliated Hospital of Anhui Medical University, The School of Mental Health and Psychological Sciences, Anhui Medical University, Hefei, 230032, China

[b] Institute of Artificial Intelligence, Hefei Comprehensive National Science Center, Hefei, 230088, China

[c] Anhui Province Key Laboratory of Cognition and Neuropsychiatric Disorders, Hefei, 230032, China.

[d] Collaborative Innovation Center of Neuropsychiatric Disorders and Mental Health, Anhui Province, 230032, China

[e] The Clinical Hospital of Chengdu Brain Science Institute, School of Life Science and Technology, University of Electronic Science and Technology of China, Chengdu, 610000, China.

[f] MOE Key Lab for Neuroinformation, High-Field Magnetic Resonance Brain Imaging Key Laboratory of Sichuan Province, University of Electronic Science and Technology of China, Chengdu, 610000, China.

[g] Department of Psychiatry, Anhui Mental Health Center, Hefei, 230022, China

[h] Institute of Neuroscience and Medicine, Brain and Behaviour (INM-7), Research Centre Jülich, Jülich, Germany.

[i] Institute of Systems Neuroscience, Medical Faculty, Heinrich Heine University

Düsseldorf, Düsseldorf, Germany.
[j] Department of Psychiatry and Medical Psychology, Ghent University, Ghent, Belgium.

#These authors equally contributed to this work.

*To whom correspondence should be addressed; The First Affiliated Hospital of Anhui Medical University, The School of Mental Health and Psychological Sciences, Anhui Medical University, No.81 Meishan Road, Shushan District, Hefei, 230032, China, e-mail: ayfytyh@126.com (Y. Tian); wangkai1964@126.com (K. Wang)

Abstract:
Electroconvulsive therapy (ECT) is an effective neuromodulatory therapy for major depressive disorder (MDD). Treatment is associated with regional changes in brain structure and function, indicating activation of neuroplastic processes. To investigate the underlying neurobiological mechanism of macroscopic reorganization following ECT, we longitudinally (before and after ECT in two centers) collected magnetic resonance images for 96 MDD patients. Similar patterns of cortical thickness (CT) changes following ECT were observed in two centers. These CT changes were spatially colocalized with a weighted combination of genes enriched for neuroplasticity-related ontology terms and pathways (e.g., synaptic pruning) as well as with a higher density of D2/3 dopamine receptors. A multiple linear regression model indicated that the region-specific gene expression and receptor density patterns explained 40% of the variance in CT changes after ECT. In conclusion, these findings suggested that dopamine signaling and neuroplasticity-related genes are associated with the ECT-induced morphological reorganization.

Key words: Electroconvulsive therapy, major depression disorder, cortical thickness, neuroplasticity, gene expression, neurotransmitter

Introduction

Electroconvulsive therapy (ECT) is a neuromodulatory and somatic therapy in severe major depressive disorder (MDD) that has not responded to drug treatment. However, despite its efficacy, the mechanism of action is largely unknown. As it may clarify the neural mechanisms of ECT, delineating brain structural correlation of response is a key clinical research goal. Structural magnetic resonance imaging (MRI) studies showed that some regions (e.g., insular and temporal lobes) were more likely to be modulated by ECT (Dukart, et al., 2014; Oltedal, et al., 2018; Pirnia, et al., 2016). Regional electric field may explain the volume change in the mesial temporal lobe (Argyelan, et al., 2019; Takamiya, et al., 2021), but the heterogeneous changes across brain regions are largely unknown. Comprehensive modeling of key factors involved in determining why brain regions heterogeneously respond to ECT could shed more light on the neuroplasticity of the human brain, and consequently may further optimize the neuromodulation protocols. According to animal and human studies, we hypothesized that the heterogeneous cortical plasticity of electroconvulsive seizures could be partially explained with genetic and neurotransmitter factors, and each is now considered in turn.

Although ECT is highly effective for patients with MDD, clinical outcome still varies in individuals (Fink, 2014). This variability has been related to the polymorphisms of some candidate genes (Benson-Martin, et al., 2016), such as the catechol-o-methyltransferase (COMT) gene (Tang, et al., 2020). Animal studies indicated that electroconvulsive seizures (ECS), a model of ECT, regulated multiple genes within distinct pathways (Altar, et al., 2004). In these preclinical studies, genes that are related to neurogenesis and neuroimmune reactions, such as brain-derived neurotrophic factor (Viikki, et al., 2013) and

interleukin-6 (van Buel, et al., 2015), were frequently reported. These ECT-induced gene expressions may be significant in fighting against neural atrophy and imflammation, both of which have been hypothesized in the pathogenesis of MDD (Galts, et al., 2019; Wittenberg, et al., 2020). These suggest that brain regions sensitive to ECT are enriched with the expression of specific genes.

Dysfunctions of several neurotransmitter systems, including serotonine, dompamine, and noradrenaline, have been hypothesized in the aetiology of depression for decades. Antidepressant drugs working on these systems can effectively alleviate depressive symptoms (Undurraga and Baldessarini, 2012). The clinical effect of ECT has also been found to be mediated by neurotransmitters (Baldinger, et al., 2014; Goodwin, et al., 1987). For instance, polymorphisms within genes encoding for dopamine and 5-hydroxytryptamine (5-HT) appeared to predict the response to ECT (Pinna, et al., 2018). This insight is equally found in observations from positron emission tomography (PET) studies in depression. After completion of ECT, the binding potential of dopamine transporters (Masuoka, et al., 2020) and serotonin receptors (Lanzenberger, et al., 2013) were decreased in brain areas having a major role in affective processes. Thus, we hypothesized that the heterogeneous distribution of neurotransmitters may play a potential role in the regional-specific plasticity to ECT.

In this work, we aimed to understand the mechanism of ECT by associating the treatment-related cortical plasticity with genetic and neurotransmitter factors. We began by deriving a robust pattern of cortical thickness (CT) changes following ECT in two independent MDD cohorts. Then, we identified genes with similar spatial expression as this neuroplasticity map using transcriptomic analyses. Functional enrichment analysis was adopted to infer the ontological pathways. Next, we determined whether the CT changes were prominent in regions with high MDD-related neurotransmitters. Finally, we combined all

these factors into a single regression model to explore the putative predictors of cortical neuroplasticity by ECT.

Results

Experiment design

We included patients diagnosed with MDD (n = 106) with longitudinal MRI and clinical data. The high-resolution structural MRI data were collected in two centers: Anhui Medical University (AHMU, n = 56), and the University of Science and Technology of China (USTC, n = 40). All patients were scanned twice: before the first (<24 h) and after the last ECT administration (72 h apart). After ~8 times of ECT, Hamilton depression scale (HAMD) score in 77 (80%) patients decreased more than 50%. No significant difference between centers was found in demographics, symptom measures, and ECT procedures (Table 1).

Neuroplasticity revealed by cortical thickness changes

After ECT, MDD patients from AHMU (n = 56) showed heterogeneous CT changes across cortical regions (with a prominent CT increase in the bilateral insula; Fig. 1A). This pattern was validated by the independent data of USTC (n = 40). These patterns of CT changes showed a highly spatial correspondence ($r_{(175)} = 0.53$, $P_{spin} < 0.0001$; Fig. 1B). We, thus, incorporated them into one model (Morgan, et al., 2019) and found that four brain regions survived the FDR correction (Fig. 1C, Table S1). Specifically, the ECT significantly increased CT in the bilateral medial parts of the superior temporal gyrus (mSTG), and bilateral insula. The CT changes of these regions did not show significant correlation with changes in HAMD ($\rho > 0.05$, FDR corrected).

Cortical gene expression and neuroplasticity

Gene expression data were collected from AHBA, a whole-brain transcriptomic dataset (see http://human.brain-map.org) (Hawrylycz, et al., 2012). The AHBA

dataset included two right-hemispheric and six left-hemispheric data. Only the later was used in the following genetic imaging analysis (Arnatkeviciute, et al., 2019). We used partial least squares (PLS) regression to determine differences between regional CT changes and gene expression (177 regions × 10,027 genes) (Fig. 2A). Following report focused on the first two PLS components (PLS1 and PLS2) which explained more than 15% of the variance (Fig. S1). Both PLS1 and PLS2 weighted gene expression maps were spatially correlated with the t-map of CT changes (PLS1: $r_{(175)} = 0.42$, $P_{spin} < 0.0001$, Fig. 2B; PLS2: $r_{(175)} = 0.41$, $P_{spin} < 0.0001$, Fig. 2C). These correlations were 'spin' corrected by randomly rotating the t map to account for spatial autocorrelation (Fulcher, et al., 2021).

We found 1,552 and 987 postively weighted genes in PLS1 and PLS2 ($Z > 3$, $P_{FDR} < 0.01$), respectively. These genes comprised a dense, topologically clustered interaction network that was enriched for several GO biological processes and KEGG pathways. The top significant terms ($P_{FDR} < 0.05$) indicated a relation with homeostasis and neuroplasticity, including "temperature homeostasis", "regulation of fever generation", "neuroactive ligand-receptor interaction", "regulation of growth" in PLS1 (Fig. 2B), and "positive regulation of cell migration", "organelle localization", "regulation of cell activation", "synaptic pruning" in PLS2 (Fig. 2C).

Neurotransmitter distribution and neuroplasticity

We concentrated on the serotonergic and dopaminergic neurotransmitter systems (Mandal, et al., 2020), given that only these were provided by the open PET data (Grecchi, et al., 2014; Savli, et al., 2012), including D2/D3 receptor, inhibitory (5-HT1A and 5-HT1B) and excitatory (5-HT2A) 5-HT receptors, and the transporter (5-HTT). These PET maps were correlated with the t-maps of the CT changes after ECT across the 180 brain regions in the left hemisphere. We found a significant spatial correspondence for the D2/D3 receptor

($r_{(178)}$=0.35, p_{spin} < 0.0001, Fig. 3) map, but not the others (Fig. S2).

Multivariate model combining genetic and neurotransmitter contributions

To examine the genetic and neurotransmitter contributions to the CT changes, we conducted multiple linear regression with the predicted measures including PLS1, PLS2, and D2/D3 receptor maps (Fig. 4A). The model explained 40% of the variance in CT changes ($F_{(3,173)}$ = 39.17, P < 2.2×10^{-16}; adjusted R^2 = 0.39; Fig. 4B). All individual factors significantly predicted the variance in CT changes (Table S2 and Fig. 4C).

Discussion

To understand the neuroplasticity changes following ECT, we associated the genetic and neurotransmitter factors with brain morphological changes in MDD patients after treatment. We found that CT changes were heterogeneous across cortices, but the global pattern was quite similar between the two independent cohorts. Brain regions showing CT increase after ECT were characterized by genes enriched for neuroplasticity-related biological processes and high density of D2/D3. Collectively, the genetic and neurotransmitter factors explained 40% of the variance in CT reorganization across cortices.

Cortical thickness changes following ECT

The structural changes of the mesial temporal lobe have been widely investigated (Gbyl and Videbech, 2018; Janouschek, et al., 2021) in ECT studies, given their importance in emotion and memory regulation. Beside these regions-of-interest (ROIs), volume alterations in neocortices were also reported by a large sample mega-analysis (Ousdal, et al., 2020). Here, we also focused on neocortices and found a highly consistent spatial pattern of CT change across two independent samples. Importantly, the significant CT increases we found in the bilateral insular and mSTG were consistently reported previously

(Gbyl, et al., 2019; Gryglewski, et al., 2019; Pirnia, et al., 2016; Sartorius, et al., 2016; van Eijndhoven, et al., 2016; Xu, et al., 2019; Yrondi, et al., 2019). These structural alterations in MRI may be associated to changes in cellular level (Kassem, et al., 2013; Keifer, et al., 2015). For instance, animal ECS studies suggested that both neural (e.g., increased dendrites and synapse) (Chen, et al., 2018; Maynard, et al., 2018) and glial (e.g., proliferation) (Madsen, et al., 2005; Ongur, et al., 2007) factors may contribute to the ECT induced CT changes. We correlated the structural changes with symptom improvement, but no significant correlation was found. A similar negative result was also reported by large sample studies (Oltedal, et al., 2018; Ousdal, et al., 2020). Together with previous network studies (Wang, et al., 2018; Xu, et al., 2020), these findings suggest that it is the interaction of the modulated regions rather than any single brain area that is more likely contributed to the symptom improvement.

Genetic determinants of morphological plasticity

The genetic mechanism of ECT has been widely investigated in animals using ECS (Benson-Martin, et al., 2016; Giacobbe, et al., 2020). Using a large sample of MDD patients, we associated the CT alterations to the expression level of ten thousand genes. PLS identified a list of positively weighted genes with high expression in cortices with increased thickness. In PLS1, the identified KEGG pathway ("neuroactive ligand-receptor interaction") in mediating the transduction of signals from the extracellular environment into cells. This pathway was associated with the modulation of synaptic plasticity and inflammation (Xiang, et al., 2019) and was related to the brain morphological abnormalities in MDD (Li, et al., 2021). The top GO biological processes ("regulation of fever generation" and "temperature homeostasis") were common immuno-inflammatory responses which could be immediately activated by ECT (Yrondi, et al., 2018). It suggested that temperature control was a necessary factor to reorganize the local neuro-system (Robertson and Money, 2012).

In PLS2, the top GO terms were neuroplasticity-related biological processes, such as the increased extent of cell migration ("positive regulation of cell migration") (Faini, et al., 2021), modulated frequency or extent of cell activation ("regulation of cell activation") (Flavell and Greenberg, 2008), and re-positioned organelle location ("organelle localization") (van Bergeijk, et al., 2016). Especially, we also found "synaptic pruning" which usually occurs in the development of the nervous system (e.g., early childhood and the onset of puberty) (Chechik, et al., 1998), but also involved in reversing a depressive behavioral state (Vose and Stanton, 2017). These findings suggested that genes supportive of neuroplasticity played a vital role in determining to what extend ECT could modulate a brain region.

Neurotransmitter effect on morphological plasticity

Based on the pathogenic hypothesis (Hirschfeld, 2000; Savitz and Drevets, 2013), standard pharmacological treatments for MDD mostly act on monoaminergic systems, such as 5-HT, noradrenaline, and dopamine. By modulating developmental cellular migration and cytoarchitecture, these neurotrasmitters were vital for the normal maturation of the neural system (Daubert and Condron, 2010; Robinson and Gradinaru, 2018). In healthy adults, the expression of dopamine receptors was correlated with cerebral morphology (Woodward, et al., 2009). This study found prominent CT increases in regions with a high density of D2/D3, suggesting the support of the dopaminergic system to the ECT induced structural plasticity. This is consistent with the preclinical and therapeutic studies (Baldinger, et al., 2014). Particularly, the treatment effect of ECT was influenced by dopamine receptor gene variation (Dannlowski, et al., 2013). On the contrary, no significant association was found between CT changes and 5-HT receptor or transporter density. This negative result should be interpreted cautiously, since only two of the multiple 5-HT receptors were included in the analysis. It will be important for future studies to

test whether the serotonergic system is involved in ECT mechanism through other types of receptors.

Methodological considerations and future directions

Several methodological issues have to be considered. First, to increase the homogeneity of participants, we only included MDD patients who received the bifrontal ECT. However, in clinical practice, the patients could be bipolar (Sanghani, et al., 2018), and the ECT protocol could be bitemporal or right unilateral (Ousdal, et al., 2020). Future studies may consider the interaction of these variables on the ECT-induced neuroplasticity. Second, the AHBA data were measured in six participants without psychiatric diagnosis. Additionally, data of the right hemisphere was only available in two participants, which has been excluded from this study. Thus, the relationship between genes and ECT-related CT changes does not represent the condition of the entire brain. Third, noradrenaline was also a vital neurotransmitter related to the aetiology of depression, and one of the target systems in drug therapy (Undurraga and Baldessarini, 2012). It is important for future studies to map the distribution of noradrenaline and estimate whether this system involved in the region-specific neuroplasticity in ECT.

Conclusion

This brain imaging study linked genetic and neurotransmitter factors to the cortical morphological plasticity induced by ECT in MDD patients. The CT changes after ECT were heterogeneous across brain regions, which can be explained by (40% variance) gene expression and the density of D2/D3. Overall, this study associated microscale factors to brain morphological plasticity, which is a vital step toward integrating multiscale mechanisms of ECT.

Methods

Participants

Patients experiencing a current depressive episode (n = 106) were included from Anhui Medical University (AHMU). According to the Diagnostic and Statistical Manual of Mental Disorders, Fourth Edition, all were diagnosed with having a current depressive episode. Patients were excluded if they met any of the following exclusion criteria: (1) a history of ECT in the last three months; (2) age > 65 years; (3) diagnosed with substance misuse, bipolar disorder, schizoaffective disorder or schizophrenia; (4) a history of neurological illness; (5) other contraindications of MRI scan and ECT administration.

ECT procedures

All patients received ECT at AHMU with a modified bifrontal ECT protocol using a Thymatron System IV Integrated ECT System (Somatics, Lake Bluff, IL). It was administered three times a week using a constant current of 0.9 A with 1.0 msec pulse width, after induction of anesthesia, intravenously with propofol, muscle relaxation with succinylcholine, and suppression of gland secretion intravenously with atropine. The initial percent energy dial was set based on the age of each participant (e.g., 50% for a 50-year-old patient). The stimulation strength was evenly adjusted with an increment of 5% of the maximum charge (approximately 1,000 millicoulombs) in our treatment strategy. If no seizure was detected with the initial stimulation setting, the percent energy was increased until the seizure was visually observed. The first three ECT administrations occurred on consecutive days, and the remaining ECT administrations were conducted every other day with a break on weekends until patients' symptoms remitted. Two independent experienced psychiatrists administered the HAMD. If patients did not remit after six sessions, treatment continued until remission was achieved or until a maximum of 12 ECT sessions have been administered. Treatment responders were defined as patients whose HAMD score decreased more than 50% after ECT.

MRI data acquisition

Structural MRI scans were obtained at two MRI scanners at the AHMU (n = 56, 3.0 T, Signa HDxt, GE Healthcare), and the University of Science and Technology of China (USTC, n = 40, 3.0 T, Discovery 750; GE Healthcare). High spatial resolution T1-weighted anatomic images were acquired in the sagittal orientation. Scanning parameters for the AHMU center are: TR repetition/echo time, 8.68/3.18 ms; flip angle = 8°; field of view = 256 × 256 mm^3; 256 × 256 matrix; slice thickness = 1 mm; voxel size = 1 × 1 × 1 mm^3, 188 sagittal orientation slices. Similar scanning parameters for the USTC center were: repetition/echo time, 8.16/3.18 ms; flip angle, 12°; field of view, 256 × 256 mm^2; 256 × 256 matrix; section thickness, 1 mm; voxel size, 1 × 1 × 1 mm^3, 188 sagittal orientation slices.

MRI data processing

The CT was computed using the standard longitudinal pipeline in FreeSurfer version 5.3 (Reuter and Fischl, 2011; Reuter, et al., 2010; Reuter, et al., 2012). Briefly, an unbiased within-subject template space and image was created using robust, inverse consistent registration. This “base” template of each participant was based on images from all time points. Then, skull stripping, Talairach coordinate transformation, and atlas registration as well as spherical surface maps and parcellations were initialized with common information from the “base” template, to minimize random error and preserve stable within-subject features across all time points. Finally, the cortical surfaces were divided into 360 regions-of-interest (ROIs) based on the HCP-MMP 1.0 atlas (Glasser, et al., 2016). The CT (Z-transformed) of these ROIs were compared between post- and pre-ECT using paired-t test. *P* values for post- and pre-ECT differences in regional CT were combined across the two samples using Fisher’s method (Morgan, et al., 2019). Significance was set at $p < 0.005$ with FDR correction for multiple comparisons across regions to control type I error.

Genetic expression

Brain-wide gene expression information was adopted from the AHBA dataset (http://human.brain-map.org) (Hawrylycz, et al., 2012), which were measured in six postmortem brains (age = 42.50 ± 13.38 years; male/female = 5/1) with 3,702 spatially distinct samples. According to Arnatkevic et al.(Arnatkeviciute, et al., 2019), six steps of preprocessing were performed as follows: (i) verifying probe-to-gene annotations using the Re-annotator toolkit (Arloth, et al., 2015); (ii) filtering of probes (intensity-based filtering) that do not exceed background noise, excluding at least 50% of all samples across participants; (iii) selecting the highest correlation to RNA-seq data; (iv) samples assignment to the HCP 360 atlas within 2 mm Euclidean distance of a parcel; (v) normalization of expression measures using a scaled robust sigmoid for each participant; and (vi) gene set filtering based on differential stability. Because of the small sample size (only 2) of the right hemispheric data, only the AHBA data of the left hemisphere was considered in our analysis. Finally, gene expression was obtained by averaging all samples from six donors, resulting in a gene expression map (177 regions × 10,027 gene expression levels).

PLS regression (Abdi, 2010) was used to determine the relationship between regional changes in cortical thickness (t-values from 177 ROIs, left hemisphere) and transcriptional activity for all 10,027 genes. It produces linear combinations of gene expression, explaining the maximum amount of variance of cortical thickness changes. We chose to focus on the first two components (PLS1 and PLS2) which explained more than 15% of the variance. Bootstrapping with 1,000 iterations was used to estimate the Z score of each gene in PLS1 and PLS2. Significant positive Z scores implicated genes that were overexpressed as increased regional thickness.

We performed enrichment of KEGG pathways and GO enrichment of biological processes for genes with $Z > 3$ (FDR corrected $P < 0.05$) at Metascape website, which provides automated meta-analysis tools to understand either common or

unique pathways in 40 independent knowledge bases. (Zhou, et al., 2019) (https://metascape.org/gp/index.html#/main/step1).

Neurotransmitter distribution

We used open source PET data from unrelated control groups to investigate the effect of neurotransmitter distribution, including D2/D3 receptor, inhibitory (5-HT1A and 5-HT1B) and excitatory (5-HT2A) 5-HT receptors, and the transporter (5-HTT). Cerebral PET scanning with [11C]raclopride tracer for D2/D3 receptor was acquired as part of a previous study (Grecchi, et al., 2014) and further details can be found elsewhere (Rizzo, et al., 2016). The 5-HT receptors and transporter templates (Savli, et al., 2012) were also available online (www.meduniwien.ac.at/neuroimaging/downloads.html). The 5-TH1A and 5-TH1B templates were averaged to represent the inhibitory 5-TH receptor map in this study. Linear correlations were performed to test the associations between the spatial pattern of cortical thickness changes and to evaluate the spatial distribution of these PET markers of dopaminergic and 5-TH function independently. The significance of correlation were corrected by the spin test ($P_{spin} < 0.05$).

Multivariate model

To determine how different factors contributed to neuroplasticity, we constructed a multiple linear regression model combining each of the factors we found to be associated with cortical thickness changes (Mandal, et al., 2020). The model included PLS1 and PLS2 loading, and dopamine D2/D3 receptor. The dependent variable for the model was to map of the cortical thickness alterations after ECT. The dependent variable and each predictor were Z-scored and averaged independently within 177 ROIs from the left hemisphere.

After determining the percentage of explained variance in cortical thickness alterations from these predictors, we explored the individual contribution of

each variable by calculating the square of the partial correlation between that variable and cortical thickness alterations. The significance of the explained variance was assessed by comparison of the distribution of explained variances between the variable and 10,000 permuted, spatially contiguous, null models of the cortical thickness alteration map (Mandal, et al., 2020).

Null models

A spin-based method was used to correct for potential confounding effects of spatial autocorrelation. The spin test is a spatial permutation method based on angular permutations of spherical projections onto the cortical surface. Specifically, we first generated 10,000 random spatial rotations (i.e., spins) of the cortical ROIs to generate a null distribution (https://github.com/frantisekvasa/rotate_parcellation) (Vasa, et al., 2018). Then, the p_{spin} values were obtained by comparison with the null model (<5th, or >95th percentile).

Acknowledgments

The authors would like to thank Information Science Laboratory Center of USTC for the measurement services and all participants. This study was funded by the National Natural Science Foundation of China, Grant Numbers: 81971689, 81771456, 91432301, 81671354, 31571149, and 31970979; the Science Fund for Distinguished Young Scholars of Anhui Province, Grant Number: 1808085J23; the National Basic Research Program of China, Grant Number: 2015CB856405; the National Key R&D Plan of China, Grant Number: 2016YFC1300604; the Collaborative Innovation Center of Neuropsychiatric Disorders and Mental Health of Anhui Province; and the Youth Top-notch Talent Support Program of Anhui Medical University.

Conflict of interest

The authors declare that they have no conflict of interest.

References:

Abdi, H. (2010) Partial least squares regression and projection on latent structure (PLS Regression). WIREs Comp. Stat., 2:9.

Altar, C.A., Laeng, P., Jurata, L.W., Brockman, J.A., Lemire, A., Bullard, J., Bukhman, Y.V., Young, T.A., Charles, V., Palfreyman, M.G. (2004) Electroconvulsive seizures regulate gene expression of distinct neurotrophic signaling pathways. The Journal of neuroscience : the official journal of the Society for Neuroscience, 24:2667-77.

Argyelan, M., Oltedal, L., Deng, Z.D., Wade, B., Bikson, M., Joanlanne, A., Sanghani, S., Bartsch, H., Cano, M., Dale, A.M., Dannlowski, U., Dols, A., Enneking, V., Espinoza, R., Kessler, U., Narr, K.L., Oedegaard, K.J., Oudega, M.L., Redlich, R., Stek, M.L., Takamiya, A., Emsell, L., Bouckaert, F., Sienaert, P., Pujol, J., Tendolkar, I., van Eijndhoven, P., Petrides, G., Malhotra, A.K., Abbott, C. (2019) Electric field causes volumetric changes in the human brain. eLife, 8.

Arloth, J., Bader, D.M., Roh, S., Altmann, A. (2015) Re-Annotator: Annotation Pipeline for Microarray Probe Sequences. PloS one, 10:e0139516.

Arnatkeviciute, A., Fulcher, B.D., Fornito, A. (2019) A practical guide to linking brain-wide gene expression and neuroimaging data. NeuroImage, 189:353-367.

Baldinger, P., Lotan, A., Frey, R., Kasper, S., Lerer, B., Lanzenberger, R. (2014) Neurotransmitters and electroconvulsive therapy. The journal of ECT, 30:116-21.

Benson-Martin, J.J., Stein, D.J., Baldwin, D.S., Domschke, K. (2016) Genetic mechanisms of electroconvulsive therapy response in depression. Hum Psychopharmacol, 31:247-51.

Chechik, G., Meilijson, I., Ruppin, E. (1998) Synaptic pruning in development: a computational account.

Neural Comput, 10:1759-77.

Chen, F., Ardalan, M., Elfving, B., Wegener, G., Madsen, T.M., Nyengaard, J.R. (2018) Mitochondria Are Critical for BDNF-Mediated Synaptic and Vascular Plasticity of Hippocampus following Repeated Electroconvulsive Seizures. The international journal of neuropsychopharmacology, 21:291-304.

Dannlowski, U., Domschke, K., Birosova, E., Lawford, B., Young, R., Voisey, J., Morris, C.P., Suslow, T., Konrad, C., Kugel, H., Ohrmann, P., Bauer, J., Schoning, S., Zavorotnyy, M., Diemer, J., Arolt, V., Baune, B.T., Zwanzger, P. (2013) Dopamine D(3) receptor gene variation: impact on electroconvulsive therapy response and ventral striatum responsiveness in depression. The international journal of neuropsychopharmacology, 16:1443-59.

Daubert, E.A., Condron, B.G. (2010) Serotonin: a regulator of neuronal morphology and circuitry. Trends in neurosciences, 33:424-34.

Dukart, J., Regen, F., Kherif, F., Colla, M., Bajbouj, M., Heuser, I., Frackowiak, R.S., Draganski, B. (2014) Electroconvulsive therapy-induced brain plasticity determines therapeutic outcome in mood disorders. Proceedings of the National Academy of Sciences of the United States of America, 111:1156-61.

Faini, G., Del Bene, F., Albadri, S. (2021) Reelin functions beyond neuronal migration: from synaptogenesis to network activity modulation. Curr Opin Neurobiol, 66:135-143.

Fink, M. (2014) What was learned: studies by the consortium for research in ECT (CORE) 1997-2011. Acta psychiatrica Scandinavica, 129:417-26.

Flavell, S.W., Greenberg, M.E. (2008) Signaling mechanisms linking neuronal activity to gene expression and plasticity of the nervous system. Annual review of neuroscience, 31:563-90.

Fulcher, B.D., Arnatkeviciute, A., Fornito, A. (2021) Overcoming false-positive gene-category enrichment in the analysis of spatially resolved transcriptomic brain atlas data. Nature communications, 12:2669.

Galts, C.P.C., Bettio, L.E.B., Jewett, D.C., Yang, C.C., Brocardo, P.S., Rodrigues, A.L.S., Thacker, J.S., Gil-Mohapel, J. (2019) Depression in neurodegenerative diseases: Common mechanisms and current treatment options. Neuroscience and biobehavioral reviews, 102:56-84.

Gbyl, K., Rostrup, E., Raghava, J.M., Carlsen, J.F., Schmidt, L.S., Lindberg, U., Ashraf, A., Jorgensen, M.B., Larsson, H.B.W., Rosenberg, R., Videbech, P. (2019) Cortical thickness following electroconvulsive therapy in patients with depression: a longitudinal MRI study. Acta psychiatrica Scandinavica, 140:205-216.

Gbyl, K., Videbech, P. (2018) Electroconvulsive therapy increases brain volume in major depression: a systematic review and meta-analysis. Acta psychiatrica Scandinavica, 138:180-195.

Giacobbe, J., Pariante, C.M., Borsini, A. (2020) The innate immune system and neurogenesis as modulating mechanisms of electroconvulsive therapy in pre-clinical studies. J Psychopharmacol, 34:1086-1097.

Glasser, M.F., Coalson, T.S., Robinson, E.C., Hacker, C.D., Harwell, J., Yacoub, E., Ugurbil, K., Andersson, J., Beckmann, C.F., Jenkinson, M., Smith, S.M., Van Essen, D.C. (2016) A multi-modal parcellation of human cerebral cortex. Nature, 536:171-178.

Goodwin, G.M., De Souza, R.J., Green, A.R. (1987) Attenuation by electroconvulsive shock and antidepressant drugs of the 5-HT1A receptor-mediated hypothermia and serotonin syndrome produced by 8-OH-DPAT in the rat. Psychopharmacology (Berl), 91:500-5.

Grecchi, E., Doyle, O.M., Bertoldo, A., Pavese, N., Turkheimer, F.E. (2014) Brain shaving: adaptive

detection for brain PET data. Phys Med Biol, 59:2517-34.

Gryglewski, G., Baldinger-Melich, P., Seiger, R., Godbersen, G.M., Michenthaler, P., Klobl, M., Spurny, B., Kautzky, A., Vanicek, T., Kasper, S., Frey, R., Lanzenberger, R. (2019) Structural changes in amygdala nuclei, hippocampal subfields and cortical thickness following electroconvulsive therapy in treatment-resistant depression: longitudinal analysis. The British journal of psychiatry : the journal of mental science, 214:159-167.

Hawrylycz, M.J., Lein, E.S., Guillozet-Bongaarts, A.L., Shen, E.H., Ng, L., Miller, J.A., van de Lagemaat, L.N., Smith, K.A., Ebbert, A., Riley, Z.L., Abajian, C., Beckmann, C.F., Bernard, A., Bertagnolli, D., Boe, A.F., Cartagena, P.M., Chakravarty, M.M., Chapin, M., Chong, J., Dalley, R.A., David Daly, B., Dang, C., Datta, S., Dee, N., Dolbeare, T.A., Faber, V., Feng, D., Fowler, D.R., Goldy, J., Gregor, B.W., Haradon, Z., Haynor, D.R., Hohmann, J.G., Horvath, S., Howard, R.E., Jeromin, A., Jochim, J.M., Kinnunen, M., Lau, C., Lazarz, E.T., Lee, C., Lemon, T.A., Li, L., Li, Y., Morris, J.A., Overly, C.C., Parker, P.D., Parry, S.E., Reding, M., Royall, J.J., Schulkin, J., Sequeira, P.A., Slaughterbeck, C.R., Smith, S.C., Sodt, A.J., Sunkin, S.M., Swanson, B.E., Vawter, M.P., Williams, D., Wohnoutka, P., Zielke, H.R., Geschwind, D.H., Hof, P.R., Smith, S.M., Koch, C., Grant, S.G.N., Jones, A.R. (2012) An anatomically comprehensive atlas of the adult human brain transcriptome. Nature, 489:391-399.

Hirschfeld, R.M. (2000) History and evolution of the monoamine hypothesis of depression. The Journal of clinical psychiatry, 61 Suppl 6:4-6.

Janouschek, H., Camilleri, J.A., Peterson, Z., Sharkey, R.J., Eickhoff, C.R., Grozinger, M., Eickhoff, S.B., Nickl-Jockschat, T. (2021) Meta-analytic Evidence for Volume Increases in the Medial Temporal Lobe After Electroconvulsive Therapy. Biological psychiatry.

Kassem, M.S., Lagopoulos, J., Stait-Gardner, T., Price, W.S., Chohan, T.W., Arnold, J.C., Hatton, S.N., Bennett, M.R. (2013) Stress-induced grey matter loss determined by MRI is primarily due to loss of dendrites and their synapses. Molecular neurobiology, 47:645-61.

Keifer, O.P., Jr., Hurt, R.C., Gutman, D.A., Keilholz, S.D., Gourley, S.L., Ressler, K.J. (2015) Voxel-based morphometry predicts shifts in dendritic spine density and morphology with auditory fear conditioning. Nature communications, 6:7582.

Lanzenberger, R., Baldinger, P., Hahn, A., Ungersboeck, J., Mitterhauser, M., Winkler, D., Micskei, Z., Stein, P., Karanikas, G., Wadsak, W., Kasper, S., Frey, R. (2013) Global decrease of serotonin-1A receptor binding after electroconvulsive therapy in major depression measured by PET. Molecular psychiatry, 18:93-100.

Li, J., Seidlitz, J., Suckling, J., Fan, F., Ji, G.J., Meng, Y., Yang, S., Wang, K., Qiu, J., Chen, H., Liao, W. (2021) Cortical structural differences in major depressive disorder correlate with cell type-specific transcriptional signatures. Nature communications, 12:1647.

Madsen, T.M., Yeh, D.D., Valentine, G.W., Duman, R.S. (2005) Electroconvulsive seizure treatment increases cell proliferation in rat frontal cortex. Neuropsychopharmacology : official publication of the American College of Neuropsychopharmacology, 30:27-34.

Mandal, A.S., Romero-Garcia, R., Hart, M.G., Suckling, J. (2020) Genetic, cellular, and connectomic characterization of the brain regions commonly plagued by glioma. Brain : a journal of neurology, 143:3294-3307.

Masuoka, T., Tateno, A., Sakayori, T., Tiger, M., Kim, W., Moriya, H., Ueda, S., Arakawa, R., Okubo, Y. (2020) Electroconvulsive therapy decreases striatal dopamine transporter binding in patients with depression: A positron emission tomography study with [(18)F]FE-PE2I. Psychiatry research.

Neuroimaging, 301:111086.

Maynard, K.R., Hobbs, J.W., Rajpurohit, S.K., Martinowich, K. (2018) Electroconvulsive seizures influence dendritic spine morphology and BDNF expression in a neuroendocrine model of depression. Brain stimulation, 11:856-859.

Morgan, S.E., Seidlitz, J., Whitaker, K.J., Romero-Garcia, R., Clifton, N.E., Scarpazza, C., van Amelsvoort, T., Marcelis, M., van Os, J., Donohoe, G., Mothersill, D., Corvin, A., Pocklington, A., Raznahan, A., McGuire, P., Vertes, P.E., Bullmore, E.T. (2019) Cortical patterning of abnormal morphometric similarity in psychosis is associated with brain expression of schizophrenia-related genes. Proceedings of the National Academy of Sciences of the United States of America, 116:9604-9609.

Oltedal, L., Narr, K.L., Abbott, C., Anand, A., Argyelan, M., Bartsch, H., Dannlowski, U., Dols, A., van Eijndhoven, P., Emsell, L., Erchinger, V.J., Espinoza, R., Hahn, T., Hanson, L.G., Hellemann, G., Jorgensen, M.B., Kessler, U., Oudega, M.L., Paulson, O.B., Redlich, R., Sienaert, P., Stek, M.L., Tendolkar, I., Vandenbulcke, M., Oedegaard, K.J., Dale, A.M. (2018) Volume of the Human Hippocampus and Clinical Response Following Electroconvulsive Therapy. Biological psychiatry, 84:574-581.

Ongur, D., Pohlman, J., Dow, A.L., Eisch, A.J., Edwin, F., Heckers, S., Cohen, B.M., Patel, T.B., Carlezon, W.A., Jr. (2007) Electroconvulsive seizures stimulate glial proliferation and reduce expression of Sprouty2 within the prefrontal cortex of rats. Biological psychiatry, 62:505-12.

Ousdal, O.T., Argyelan, M., Narr, K.L., Abbott, C., Wade, B., Vandenbulcke, M., Urretavizcaya, M., Tendolkar, I., Takamiya, A., Stek, M.L., Soriano-Mas, C., Redlich, R., Paulson, O.B., Oudega, M.L., Opel, N., Nordanskog, P., Kishimoto, T., Kampe, R., Jorgensen, A., Hanson, L.G., Hamilton, J.P., Espinoza, R., Emsell, L., van Eijndhoven, P., Dols, A., Dannlowski, U., Cardoner, N., Bouckaert, F., Anand, A., Bartsch, H., Kessler, U., Oedegaard, K.J., Dale, A.M., Oltedal, L., Gemric. (2020) Brain Changes Induced by Electroconvulsive Therapy Are Broadly Distributed. Biological psychiatry, 87:451-461.

Pinna, M., Manchia, M., Oppo, R., Scano, F., Pillai, G., Loche, A.P., Salis, P., Minnai, G.P. (2018) Clinical and biological predictors of response to electroconvulsive therapy (ECT): a review. Neuroscience letters, 669:32-42.

Pirnia, T., Joshi, S.H., Leaver, A.M., Vasavada, M., Njau, S., Woods, R.P., Espinoza, R., Narr, K.L. (2016) Electroconvulsive therapy and structural neuroplasticity in neocortical, limbic and paralimbic cortex. Translational psychiatry, 6:e832.

Reuter, M., Fischl, B. (2011) Avoiding asymmetry-induced bias in longitudinal image processing. NeuroImage, 57:19-21.

Reuter, M., Rosas, H.D., Fischl, B. (2010) Highly accurate inverse consistent registration: a robust approach. NeuroImage, 53:1181-96.

Reuter, M., Schmansky, N.J., Rosas, H.D., Fischl, B. (2012) Within-subject template estimation for unbiased longitudinal image analysis. NeuroImage, 61:1402-18.

Rizzo, G., Veronese, M., Expert, P., Turkheimer, F.E., Bertoldo, A. (2016) MENGA: A New Comprehensive Tool for the Integration of Neuroimaging Data and the Allen Human Brain Transcriptome Atlas. PloS one, 11:e0148744.

Robertson, R.M., Money, T.G. (2012) Temperature and neuronal circuit function: compensation, tuning and tolerance. Curr Opin Neurobiol, 22:724-34.

Robinson, J.E., Gradinaru, V. (2018) Dopaminergic dysfunction in neurodevelopmental disorders: recent

advances and synergistic technologies to aid basic research. Curr Opin Neurobiol, 48:17-29.

Sanghani, S.N., Petrides, G., Kellner, C.H. (2018) Electroconvulsive therapy (ECT) in schizophrenia: a review of recent literature. Current opinion in psychiatry, 31:213-222.

Sartorius, A., Demirakca, T., Bohringer, A., Clemm von Hohenberg, C., Aksay, S.S., Bumb, J.M., Kranaster, L., Ende, G. (2016) Electroconvulsive therapy increases temporal gray matter volume and cortical thickness. Eur Neuropsychopharmacol, 26:506-17.

Savitz, J.B., Drevets, W.C. (2013) Neuroreceptor imaging in depression. Neurobiology of disease, 52:49-65.

Savli, M., Bauer, A., Mitterhauser, M., Ding, Y.S., Hahn, A., Kroll, T., Neumeister, A., Haeusler, D., Ungersboeck, J., Henry, S., Isfahani, S.A., Rattay, F., Wadsak, W., Kasper, S., Lanzenberger, R. (2012) Normative database of the serotonergic system in healthy subjects using multi-tracer PET. NeuroImage, 63:447-59.

Takamiya, A., Bouckaert, F., Laroy, M., Blommaert, J., Radwan, A., Khatoun, A., Deng, Z.D., Mc Laughlin, M., Van Paesschen, W., De Winter, F.L., Van den Stock, J., Sunaert, S., Sienaert, P., Vandenbulcke, M., Emsell, L. (2021) Biophysical mechanisms of electroconvulsive therapy-induced volume expansion in the medial temporal lobe: A longitudinal in vivo human imaging study. Brain stimulation, 14:1038-1047.

Tang, Z., Zhang, S., Guo, D., Wang, H. (2020) Association between COMT gene Val108/158Met and antidepressive treatment response: A meta-analysis. Gene, 734:144333.

Undurraga, J., Baldessarini, R.J. (2012) Randomized, placebo-controlled trials of antidepressants for acute major depression: thirty-year meta-analytic review. Neuropsychopharmacology : official publication of the American College of Neuropsychopharmacology, 37:851-64.

van Bergeijk, P., Hoogenraad, C.C., Kapitein, L.C. (2016) Right Time, Right Place: Probing the Functions of Organelle Positioning. Trends Cell Biol, 26:121-134.

van Buel, E.M., Patas, K., Peters, M., Bosker, F.J., Eisel, U.L., Klein, H.C. (2015) Immune and neurotrophin stimulation by electroconvulsive therapy: is some inflammation needed after all? Translational psychiatry, 5:e609.

van Eijndhoven, P., Mulders, P., Kwekkeboom, L., van Oostrom, I., van Beek, M., Janzing, J., Schene, A., Tendolkar, I. (2016) Bilateral ECT induces bilateral increases in regional cortical thickness. Translational psychiatry, 6:e874.

Vasa, F., Seidlitz, J., Romero-Garcia, R., Whitaker, K.J., Rosenthal, G., Vertes, P.E., Shinn, M., Alexander-Bloch, A., Fonagy, P., Dolan, R.J., Jones, P.B., Goodyer, I.M., consortium, N., Sporns, O., Bullmore, E.T. (2018) Adolescent Tuning of Association Cortex in Human Structural Brain Networks. Cereb Cortex, 28:281-294.

Viikki, M.L., Jarventausta, K., Leinonen, E., Huuhka, M., Mononen, N., Lehtimaki, T., Kampman, O. (2013) BDNF polymorphism rs11030101 is associated with the efficacy of electroconvulsive therapy in treatment-resistant depression. Psychiatr Genet, 23:134-6.

Vose, L.R., Stanton, P.K. (2017) Synaptic Plasticity, Metaplasticity and Depression. Curr Neuropharmacol, 15:71-86.

Wang, J., Wei, Q., Wang, L., Zhang, H., Bai, T., Cheng, L., Tian, Y., Wang, K. (2018) Functional reorganization of intra- and internetwork connectivity in major depressive disorder after electroconvulsive therapy. Human brain mapping, 39:1403-1411.

Wittenberg, G.M., Greene, J., Vertes, P.E., Drevets, W.C., Bullmore, E.T. (2020) Major Depressive Disorder Is Associated With Differential Expression of Innate Immune and Neutrophil-Related Gene

Networks in Peripheral Blood: A Quantitative Review of Whole-Genome Transcriptional Data From Case-Control Studies. Biological psychiatry, 88:625-637.

Woodward, N.D., Zald, D.H., Ding, Z., Riccardi, P., Ansari, M.S., Baldwin, R.M., Cowan, R.L., Li, R., Kessler, R.M. (2009) Cerebral morphology and dopamine D2/D3 receptor distribution in humans: a combined [18F]fallypride and voxel-based morphometry study. NeuroImage, 46:31-8.

Xiang, X., Yu, Y., Tang, X., Chen, M., Zheng, Y., Zhu, S. (2019) Transcriptome Profile in Hippocampus During Acute Inflammatory Response to Surgery: Toward Early Stage of PND. Front Immunol, 10:149.

Xu, J., Wang, J., Bai, T., Zhang, X., Li, T., Hu, Q., Li, H., Zhang, L., Wei, Q., Tian, Y., Wang, K. (2019) Electroconvulsive Therapy Induces Cortical Morphological Alterations in Major Depressive Disorder Revealed with Surface-Based Morphometry Analysis. International journal of neural systems, 29:1950005.

Xu, J., Wei, Q., Bai, T., Wang, L., Li, X., He, Z., Wu, J., Hu, Q., Yang, X., Wang, C., Tian, Y., Wang, J., Wang, K. (2020) Electroconvulsive therapy modulates functional interactions between submodules of the emotion regulation network in major depressive disorder. Translational psychiatry, 10:271.

Yrondi, A., Nemmi, F., Billoux, S., Giron, A., Sporer, M., Taib, S., Salles, J., Pierre, D., Thalamas, C., Rigal, E., Danet, L., Pariente, J., Schmitt, L., Arbus, C., Peran, P. (2019) Grey Matter changes in treatment-resistant depression during electroconvulsive therapy. Journal of affective disorders, 258:42-49.

Yrondi, A., Sporer, M., Peran, P., Schmitt, L., Arbus, C., Sauvaget, A. (2018) Electroconvulsive therapy, depression, the immune system and inflammation: A systematic review. Brain stimulation, 11:29-51.

Zhou, Y., Zhou, B., Pache, L., Chang, M., Khodabakhshi, A.H., Tanaseichuk, O., Benner, C., Chanda, S.K. (2019) Metascape provides a biologist-oriented resource for the analysis of systems-level datasets. Nature communications, 10:1523.

Table 1 Demographical and clinical characteristics of the MDD patients

	USTC cohort	AHMU cohort	Statistics	P-value
Age (years)	40.8 (12.1)	39.3 (12.1)	0.6[a]	0.54
Sex (male/female)	12/44	13/27	1.5[b]	0.22
Education (years)	9.6 (5.0)	8.1 (4.4)	1.6[a]	0.11
Age at onset (years)	35.7 (11.3)	33.7 (12.7)	0.8[a]	0.43
NO. of ECT	8.4 (1.4)	7.8 (1.4)	1.9[a]	0.07
HAMD baseline	24.0 (6.3)	22.5 (4.3)	1.4[a]	0.17
HAMD after ECT	6.8 (5.6)	5.4 (4.8)	1.2[a]	0.24
Responders/non-responders	45/11	32/8	0.002[b]	0.97

Note: Data are presented as means (standard deviations). The cohort size was obtained after the image data quality control.

Abbreviations: AHMU, Anhui Medical University; ECT, electroconvulsive therapy; HAMD, Hamilton depression scale; USTC, University of Science and Technology of China.

[a]Two-sample t-test (two-sided), [b]Chi-square test.

Figure legends:

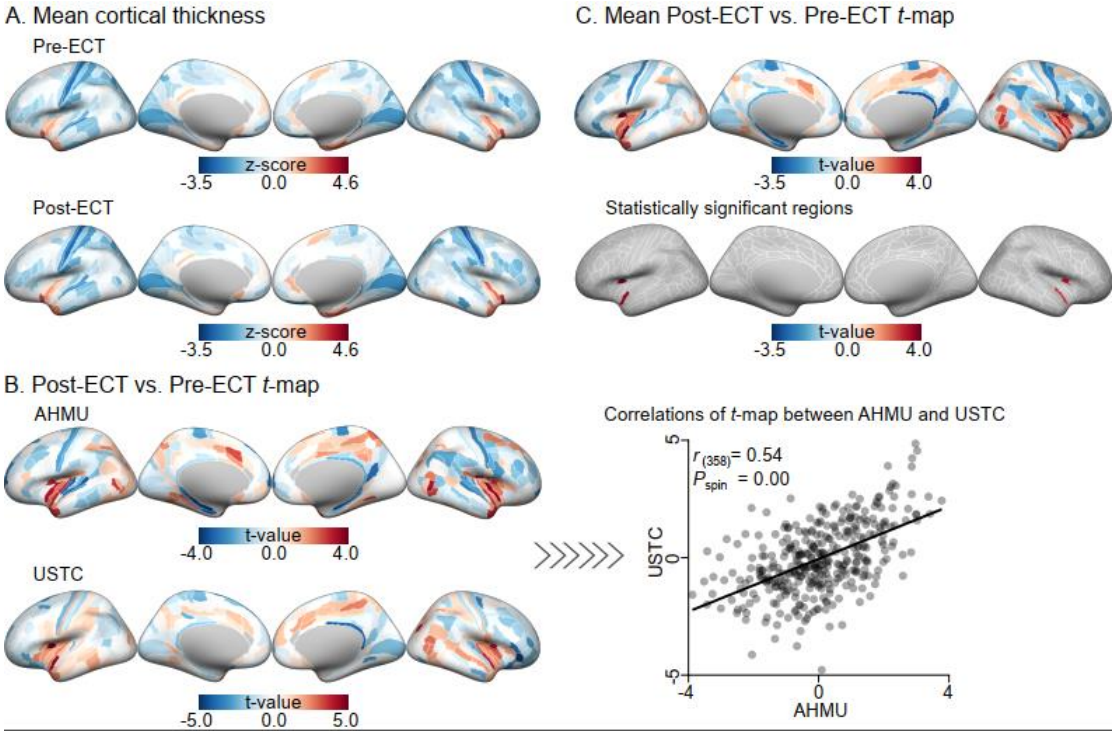

Figure 1. Cortical thickness changes after ECT. Mean cortical thickness of pre- and post-ECT conditions (A). The pattern of cortical thickness changes is similar between centers (B). Pooling the two datasets together, significant changes are found in the bilateral insular and superior temporal gyrus (C).

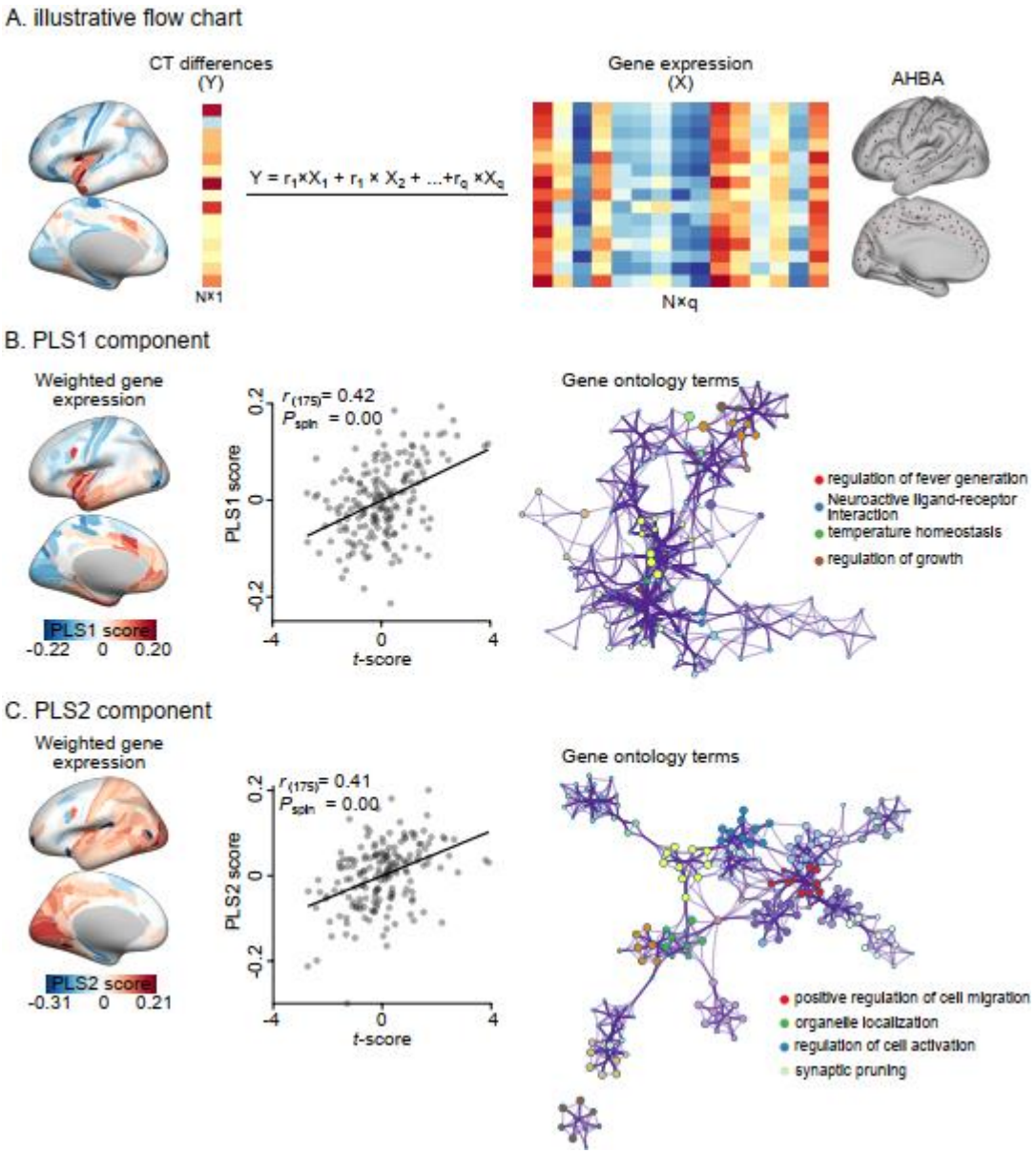

Figure 2. Gene expression profiles related to cortical thickness changes. Gene expression profiles from the Allen Human Brain Atlas in 177 regions (left hemisphere only) were averaged across six postmortem brains. Partial least squares (PLS) regression was then used to identify imaging-transcriptomic associations (A). The weighted gene expression maps of regional PLS1 (B) and PLS2 (C) scores in the left hemisphere (unthresholded). Metascape enrichment network visualization showing the intra-cluster and inter-cluster similarities of enriched terms. Each term is represented by a circle node, where its size is proportional to the number of input genes included in that term, and its color represents its cluster identity.

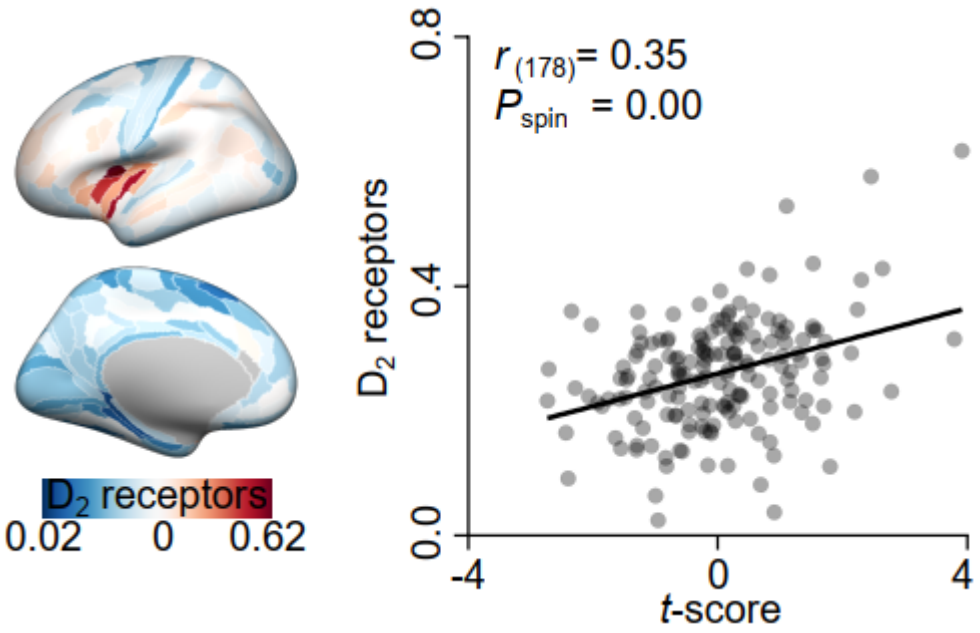

Figure 3. Dopamine receptor and cortical thickness changes. Brain map showing the spatial distribution of D2/D3 receptors. The spatial pattern across the 180 brain regions in the left hemisphere is significantly correlated with the cortical thickness changes.

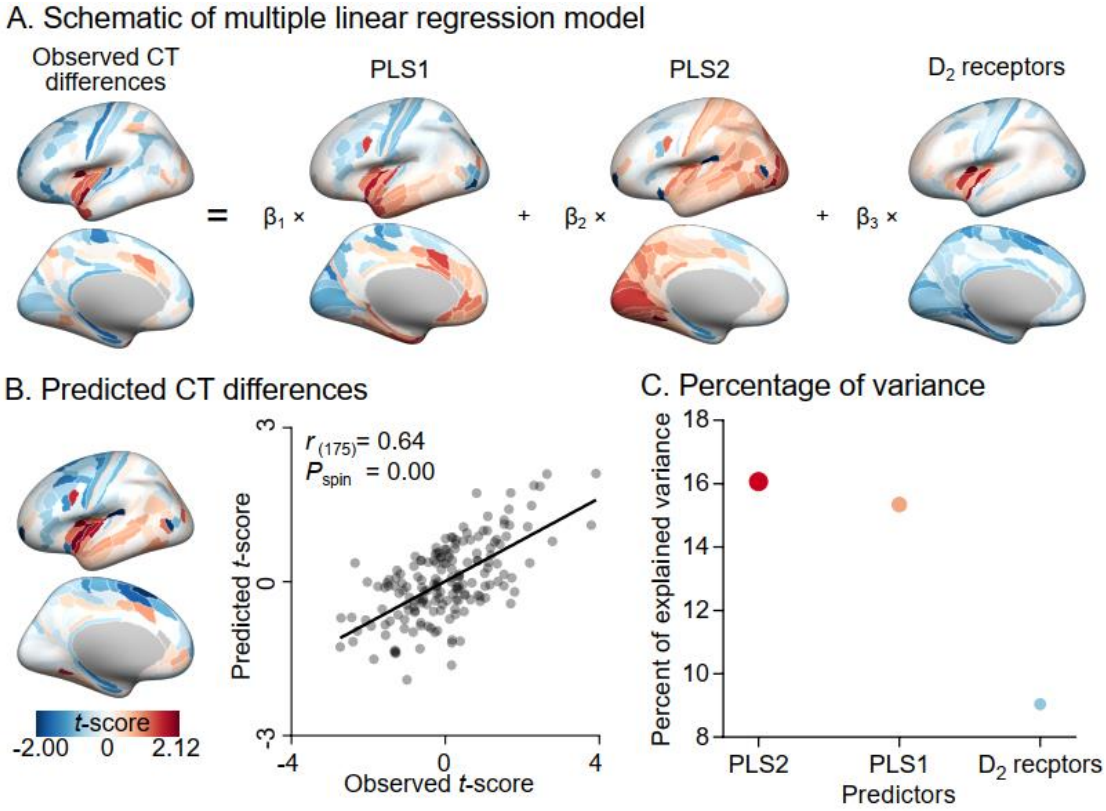

Figure 4. Multiple linear regression model relating genetic/dopamine factors with cortical thickness changes. Schematic of the multiple linear regression model (A). Intercept and error terms are not displayed. Fitted map of cortical

thickness changes, and scatter plot of predicted versus observed values (B). Percent of variance explained by each individual predictor. These values were calculated using the partial correlation coefficient between each measure and CT changes (C).